Journal of Luminescence 193 (2018) 98–105

Contents lists available at ScienceDirect

Journal of Luminescence

journal homepage: www.elsevier.com/locate/jlumin

Synthesis and photoluminescence properties of [Eu(dbm)$_3$·PX] and [Eu(acac)$_3$·PX] complexes

Thelma A. Kovacs[a], Maria Cláudia F.C. Felinto[a,*], Tiago B. Paolini[b], Bakhat Ali[a,e], Liana K.O. Nakamura[a,f], Ercules E.S. Teotonio[c], Hermi F. Brito[b,*], Oscar L. Malta[c,d]

[a] Instituto de Pesquisas Energéticas e Nucleares, Travessa R, 400 Cidade Universitária, 05508-970 São Paulo, SP, Brazil
[b] Departamento de Química Fundamental, Instituto de Química da Universidade de São Paulo, 05508-900 São Paulo, SP, Brazil
[c] Departamento de Química-Universidade Federal da Paraíba, 58051-970 João Pessoa, PB, Brazil
[d] Departamento de Química Fundamental, Universidade Federal de Pernambuco, Cidade Universitária, 50670-901 Recife, PE, Brazil
[e] Department of Chemistry, Khwaja Fareed University of Engineering and Information Technology, Rahim Yar Khan 64200, Pakistan
[f] Brazilian Synchrotron Light Laboratory (LNLS), Brazilian Center of Research in Energy and Materials (CNPEM), Campinas BR-13083-970, Brazil

ARTICLE INFO

Keywords:
Europium complexes
β-diketonates
Piroxicam (PX)
Luminescence
Experimental intensity parameters

ABSTRACT

Two novel luminescent europium *tris*(β-diketonate) complexes [Eu(dbm)$_3$·PX] and [Eu(acac)$_3$·PX] (dbm: dibenzoylmethane, acac: acetylacetonate and PX: piroxicam) were successfully synthesized. These coordination compounds were characterized by infrared vibrational spectroscopy (IR), X-ray diffraction (XRD), scanning electron microscopy (SEM), thermogravimetric analysis (TGA) and luminescence spectroscopy. The thermal behavior of the complexes was investigated by thermogravimetric analysis (TG) and differential thermogravimetric analysis (DTG) techniques. The optical results have shown that these complexes present a clear intra and inter-molecular energy transfer and corroborates the sensitivity of their emission efficiency to the excitation wavelength, multiphonon non-radiative decays and temperature dependence. These new complexes may act as efficient light converting molecular devices, suggesting that they can be used for controllable photonic applications.

1. Introduction

Lanthanide complexes possess several peculiarities for practical applications in the photonic area due to their unique photophysical properties [1–3]. The use of these coordination compounds to optimize the performance of solar cells and biomarkers has been recognized and exploited, in the last decades, once they can act as efficient convertors of ultraviolet radiation into visible light without damaging the compound in certain cases [4–9].

In the last decades, the luminescent properties of trivalent lanthanide (Ln^{3+}) complexes with a variety of organic ligands have been reported [10]. Especially luminescent Eu^{3+} materials have attracted great interest of researchers owing to their special energy level structure, sharp emission quasi-lines and in many cases very intense red emission peaks. These narrow emission quasi-lines are assigned to 4f–4f electronic transitions of Eu^{3+} ions. Usually, the effective intramolecular energy transfer takes place from the lower excited triplet state (T_1) of the ligands to the $^5D_1$ and $^5D_0$ excited levels of the Eu^{3+} ions, following strong UV absorption by the ligands (sensitizer) leading to efficient emission intensity by the metal ion [11–15].

The hydrated *Tris*(β-diketonate) complexes of Ln^{3+} have the general formula [Ln(β-diketonate)$_3$(H_2O)$_x$]. The coordinating water molecules can be replaced by other types of ligands (usually organic ligands). The introduction of an ancillary ligand can significantly improve their photoluminescence properties, due to an additional energy transfer pathway from the secondary ligand to the primary ligand or to the Ln^{3+} central ion [16]. Furthermore, it has been found that the ancillary ligand greatly affect the solubility of the corresponding complexes [9]. When Eu^{3+} complexes have water molecules as ligand, the intensity of luminescence is significantly quenched by multiphonon decay process involving O–H oscillators. Alternatively, when water molecules are replaced by organic ligands such as heterocyclic, sulfoxide, amide, phosphine oxide, the intrinsic emission efficiency (labeled as η or Q_{Ln}^{Ln}) may eventually increase, depending on the type of the ligand, as well as on the volatility, thermal stability, and carrier transport to electroluminescence devices [17].

In this work, it was utilized piroxicam (PX: 4-Hydroxy-2-methyl-N-(2-pyridinyl)-2H-1,2-benzothiazine-3-carboxamide 1,1-dioxide), as the ancillary ligand, and as the first ligand dibenzoylmethanate (dbm) or acetylacetonate (acac), yielding also to the synthesized [Eu(acac)$_3$·PX]

* Corresponding authors.
E-mail address: mfelinto@ipen.br (M.C.F.C. Felinto).

http://dx.doi.org/10.1016/j.jlumin.2017.09.029
Received 2 May 2017; Received in revised form 11 September 2017; Accepted 12 September 2017
Available online 02 October 2017
0022-2313/

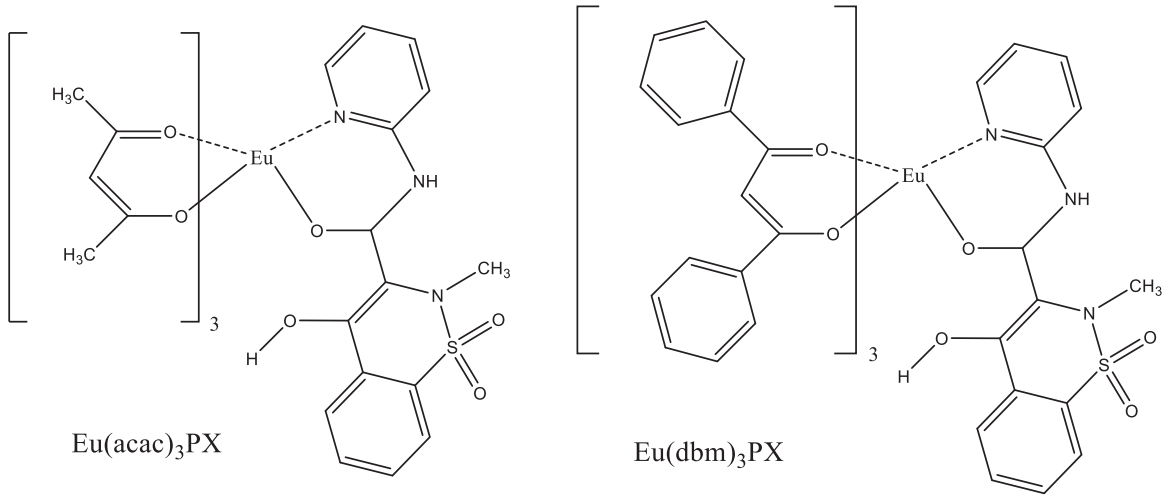

Fig. 1. Molecular structures of the [Eu(acac)$_3$·PX] and [Eu(dbm)$_3$·PX] complexes.

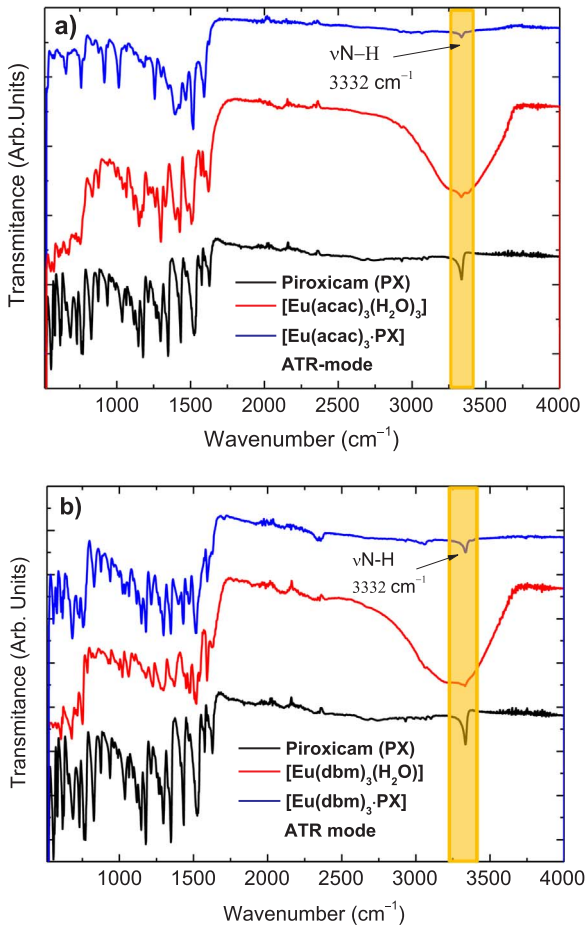

Fig. 2. Infrared absorption spectra of a) Piroxicam (PX), [Eu(acac)$_3$·PX] and [Eu(acac)$_3$(H$_2$O)$_3$] and b) Piroxicam (PX), [Eu(dbm)$_3$·PX] and [Eu(dbm)$_3$H$_2$O].

and [Eu(dbm)$_3$·PX] complexes [18]. As far as PX is concerned, it is a non-steroidal anti-inflammatory drug (NSAIDs), characterized by rapid and complete uptake in the blood stream and thus possessing a fast analgesic action [19]. They also show chemopreventive and chemosuppressive effects in different cancers such as colon, lung, breast, and human oral epithelial [19]. It is quickly absorbed by the organism, facilitating its use in the body as a biomarker.

So far, only few works containing the PX ligand and lanthanide ions have been reported in the literature [20–22]. However, a large number of studies have been concerned with Eu^{3+}-β-diketonate complexes (dbm and acac) [23]. To the best of our knowledge, no work has reported on the [Eu(dbm)$_3$·PX] and [Eu(acac)$_3$·PX] complexes (Fig. 1). Herein, we report the preparation and characterization of the complexes by using different techniques such as: IR absorption spectroscopy, XRD, SEM and photoluminescence. The TG and DTA thermal behavior of the complexes is studied to elucidate their thermal stability via mass loss. Besides, the photostability [24] and thermal stability are crucial parameters when one envisages the use in solar cells. These luminescence complexes, thermally and photostable may also act as emitting layers in organic light emitting diodes (OLEDs), as markers in biological assays, due to its easy functionality to conjugate to biological systems, and other photonic systems including lanthanide complexes thin film coatings, photo and thermally stable, in solar cells.

2. Experimental

2.1. Synthesis

Europium oxide (99.99%, Eu_2O_3), acetylacetone (98.0%, $C_5H_8O_2$) and dibenzoylmethane (≥ 98% $C_{15}H_{12}O_2$) were purchased from Sigma-Aldrich and were used without further purification. Acetone, ethanol and other substances were also used as purchased. The europium chloride $EuCl_3{\cdot}(H_2O)_6$ was prepared from its respective oxide (CSTARM, 99.99%) by salts by reaction with concentrated HCl solution until total decomposition (ca. 60–80 °C) of the solid and final pH close to 6.

The [Eu(acac)$_3$(H$_2$O)$_3$] solid complex was prepared using an equal volumes of a 0.01 mM aqueous solution of $EuCl_3(H_2O)_6$ and a 0.03 mM ethanolic solution of acetylacetonate, which was prepared by adding concentrated ammonium hydroxide to a acetylacetone solution. The ammonium acetylacetonate solution was added slowly to the lanthanide chloride solution under continuous stirring and the pH of the mixture was kept between 6 and 7 during the reaction. The yellowish crystalline precipitate was filtered and washed several times with distillated water. The obtained raw product was crystallized in acetone solvent. The pure product obtained, after repeated crystallization, was dried in a desiccator at reduced pressure until complete drying.

In case of the synthesis of the [Eu(dbm)$_3$(H$_2$O)] complex, the europium chloride aqueous solution (2.00 g, 5.46 mmol) was added to the ethanolic solution of dibenzoylmethane (3.67 g, 16.37 mmol) in molar ration 1:3 (Eu:dbm). Subsequently, the pH was adjusted to 6.5 using a 5.0 mol L^{-1} NaOH solution. The formed yellowish precipitate was filtered, washed with 50 mL of ethanol, recrystallized with acetone, and was dried in a desiccator at reduced pressure [25,26].

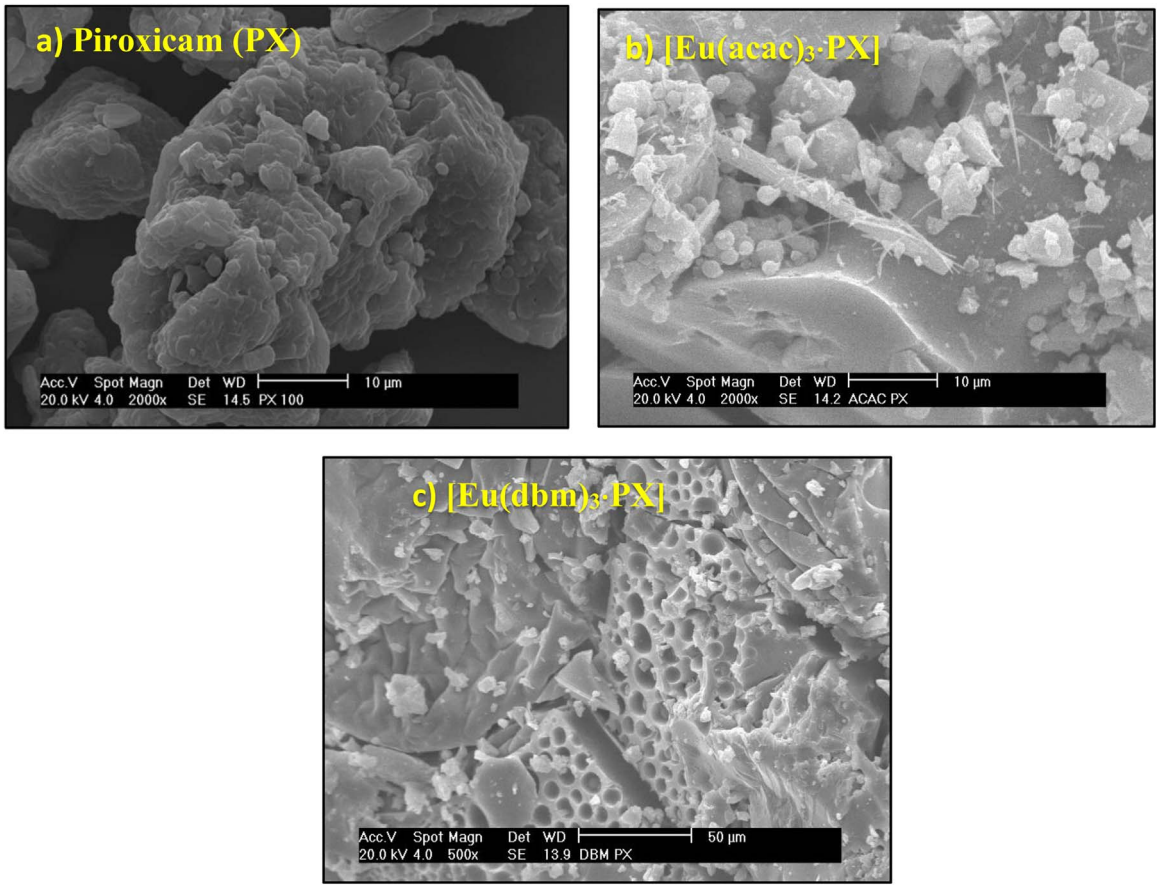

Fig. 3. SEM images of a) Piroxicam (PX), b) [Eu(acac)$_3$·PX] and c) [Eu(dbm)$_3$·PX] compounds.

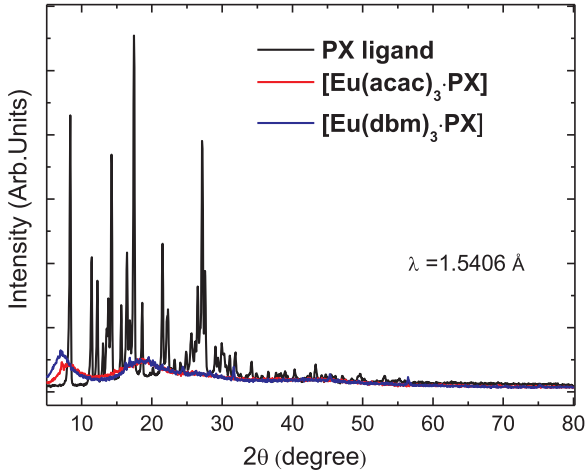

Fig. 4. X-ray diffraction patterns of the PX ligand (black line), [Eu(acac)$_3$·PX] (red line) and [Eu(dbm)$_3$·PX] (blue line). (For interpretation of the references to color in this figure legend, the reader is referred to the web version of this article.)

The [Eu(acac)$_3$·PX] and [Eu(dbm)$_3$·PX] complexes were prepared from the aforementioned hydrated complexes, according to the following procedure: an ethanolic solution of europium β-diketonate (20 mL, 1 mmol) and was added to an ethanolic-water solution of piroxicam (20 mL, 2 mmol); no heat was necessary. The resulting yellowish solution was stirred for approximately 3 h and the precipitate was formed. The solid compounds were filtered, washed with ethanol and dried in a desiccator at reduced pressure. The prepared solid complexes are stable at room temperature (300 K), insoluble in water, partially soluble in methanol and acetone and soluble in the dimethylformamide (DMF) solvents.

2.2. Apparatus

The IR absorption spectra obtained on a Thermo Scientific Nicolet 6700 FT-IR, Smart Orbit, Diamond; Class 1 laser product, by Attenuated Total Reflectance (ATR), were recorded in spectral range from 4000 to 500 cm^{-1}.

The morphology of the complexes was determined by scanning electron microscopy (SEM) with a scanning electronic microscopy Philips model XR-30. After being comminuted, the samples were deposited on a suitable metallic support and were coated with gold by sputtering technique.

XPD patterns were recorded by a Rigaku Miniflex II diffractometer in a Cu Kα radiation (λ = 1.5406 Å) from 4° to 80° (2θ). The data were processed using the MiniFlexII software.

Thermogravimetric analyses (TG and DTG) were performed by using a thermobalance SDTA-822 (Mettler Toledo) under a uniform airflow rate of 50 mL min^{-1} in the temperature interval from 32 to 974 °C, with a heating rate of 10 °C min^{-1}.

The photoluminescence study was based on the excitation and emission spectra recorded at room (300 K) and liquid nitrogen (77 K) temperatures using front face data collection mode (22.5°), with a 450 W Xenon lamp as excitation source coupled to a SPEX-Fluorolog 2 spectrometer with double monochromators. The luminescence decay curves of the complexes were recorded also at room and liquid nitrogen temperatures by using a Horiba Jobin Yvon Fluorolog-3 spectrofluorometer with both excitation and emission double grating 0.22 m monochromators, and a photomultiplier R928P PMT as detector operating on the phosphorescence mode with pulsed with a 150 W Xenon lamp as excitation source. This luminescence instrument was fully

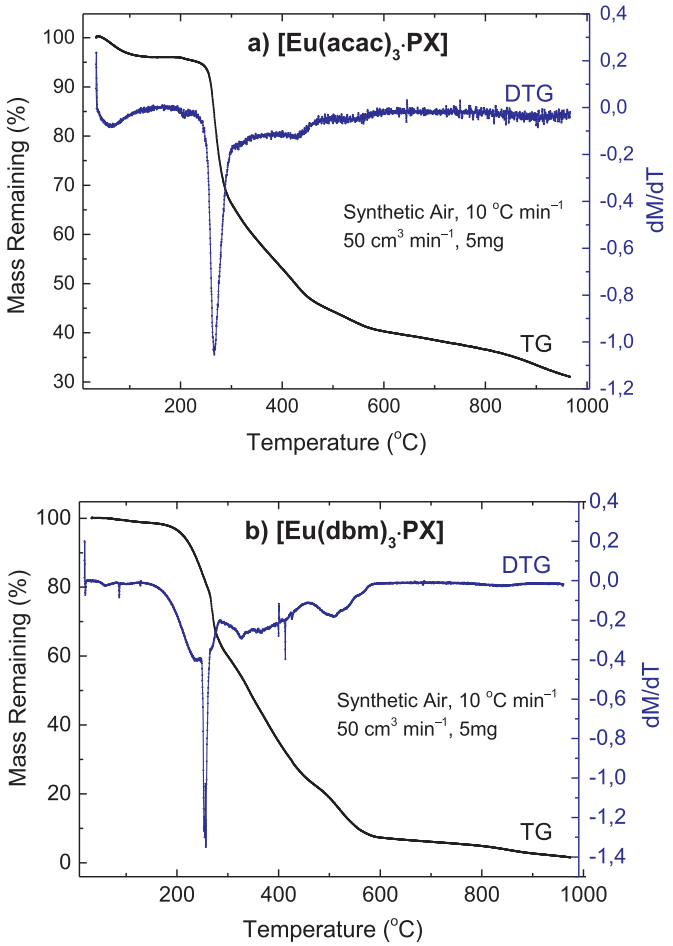

Fig. 5. The TG and DTG curves of the a) [Eu(acac)$_3$·PX] and b) [Eu(dbm)$_3$·PX] complexes.

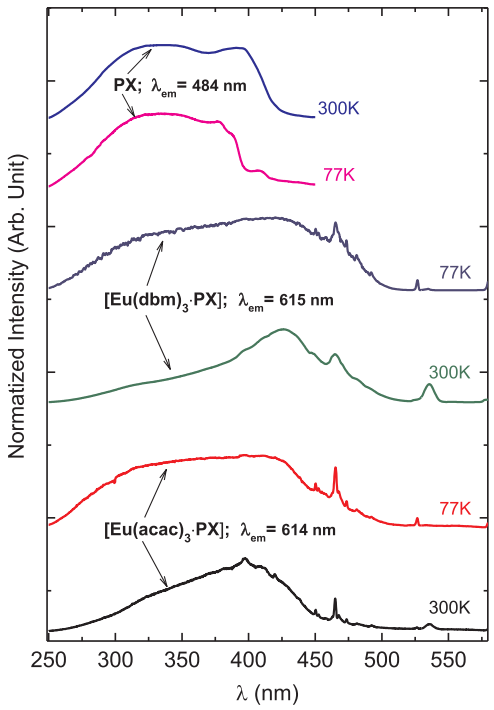

Fig. 6. Excitation spectra of PX, [Eu(acac)$_3$·PX] and [Eu(dbm)$_3$·PX] compounds recorded at 300 and 77K temperatures, under emission at 484nm (PX), 614nm (acac) and 615 nm (dbm) assigned to the $^5D_0 \rightarrow {}^7F_2$ transition of the Eu^{3+} ion.

controlled by the FluorEssence program. All luminescence data were obtained with samples contained in quartz tubes with 1 mm diameter.

3. Results and discussion

Elemental analysis (H and C %) of the chemical compositions of the [Eu(acac)$_3$·PX] and [Eu(dbm)$_3$·PX] complexes indicates that the 1:1 M ratio between the [Eu(β-diketonate)$_3$(H_2O)] and the PX ligand. For the [Eu(acac)$_3$·PX] complex – calcd: C, 46.22; H, 4.27; Eu, 19.49%; found: C, 46.04; H, 0.88, Eu, % 19.52. For [Eu(dbm)$_3$·PX] – calcd: C, 62.55; H, 3.94; Eu, 13.19%; found: C, 61.89; H, 4.01; Eu, 13.30%.

Fig. 2 depicts the FTIR spectra of the piroxicam (PX) ligand, [Eu(acac)$_3$(H_2O)], [Eu(dbm)$_3$(H_2O)], [Eu(acac)$_3$·PX] and [Eu(dbm)$_3$·PX] complexes. The IR absorption spectral data of the hydrated tris β-diketonate europium complexes presented a displacement of the CO stretching from 1560 cm^{-1} [27] in the free dbm ligand to 1517 cm^{-1} for the hydrated dbm complex and 1519 cm^{-1} for [Eu(dbm)$_3$·PX], and 1624 cm^{-1} [28] for free acac ligand, 1621–1590 cm^{-1} for the hydrated acac complex and 1593 cm^{-1} for [Eu(acac)$_3$·PX], suggesting that this ligand is coordinated to the rare earth ion through the oxygen atoms.

The IR absorption spectrum of the PX ligand (Fig. 2) shows a well defined peak at 3332 cm^{-1} and is assigned to the (N–H) vibration. In the wavenumber range 1700–1000 cm^{-1}, some of the most characteristic bands of these groups were found. The so-called amide I band, which represents mainly the ν(C=O) stretching mode, presents a very strong absorption band at 1627 cm^{-1} in free PX. In the PX complexes, this band is shifted to higher or lower frequencies or disappear, supporting the participation of the amide carbonyl group of PX in the coordination to the metal ion [29–34].

Scanning electron microscopy (SEM) images showing the morphologies of the PX ligand, [Eu(acac)$_3$·PX] and [Eu(dbm)$_3$·PX] complexes are reported (Fig. 3). Aquino et al. [25] have reported that PX might be crystallize into both needle (α) and cubic (β) form, and interestingly, both were observed. Enrichi et al. [26] reported that the Eu(acac)$_3$ complex are quite irregular in shape, partially aggregated, with a size around 500–800 nm and sponge-like. Zaharieva et al. observed that the Eu(dbm)$_3$ complex have shapeless particles from 200 nm up to a few micrometers, prismatic crystals 1–10 μm in length and 1 μm in thickness, rather specific needle (0.2 × few tens micrometers) or long-length-leaf - like particles (~ ten – few tens micrometers) and rods ~ 10 μm in diameter [35].

Upon careful observations, these complexes are formed by multiple shapes. The boundaries of these particles are not very clear because they look very aggregate, which may be caused by the PX attachment. Although some free dots with several nanometers are observed, most of them have been incorporated in large spheres. This irregular morphology and bigger size could be a disadvantage for applications as nanomarkers, which requires particles in the nanoscale [26]. Nevertheless, these particles reveal highly crystalline forms with diameters of about 10–50 μm, which may be useful to fabricate solid devices.

X-ray powder diffraction pattern (Fig. 4, black line) confirmed that the piroxicam ligand is very crystalline. On the other hand, [Eu(dbm)$_3$·PX] and [Eu(acac)$_3$·PX] complexes did not show any crystalline diffraction pattern of PX, indicating that it has made a coordination with the Eu complex leaving behind no un-wanted PX [35]. XRD pattern of the complexes correspond to the amorphous nature with the three characteristic crystalline peaks of the complex. This is probably due to excess of PX associated with the Eu^{3+} complexes (it indicates that PX tightly bounds the Eu^{3+} ion removing all water molecules from the hydrated complexes). This PX coordination in the complexes depicts a change in the crystalline structure, which strongly influences the thermal and optical properties of the complex. XRD patterns of these europium complexes indicate that the PX ligand is coordinated to the Eu^{3+} ion [36].

Thermal analysis TG/DTG curves has been used to characterize the thermal stability of the complexes (Fig. 5). In the DTG curve, we can

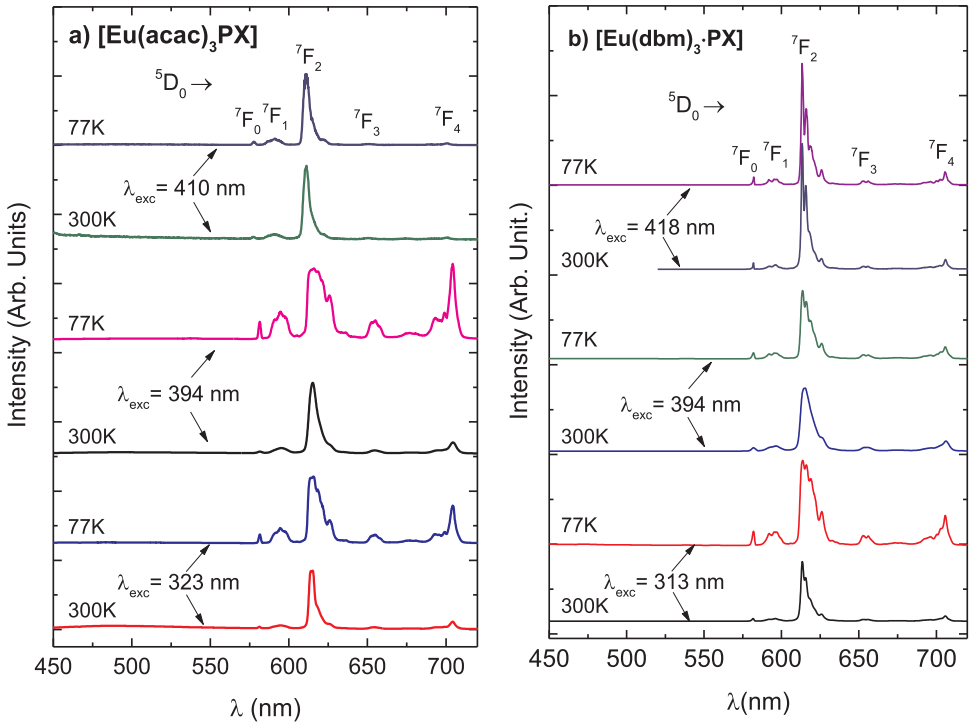

Fig. 7. Emission spectra of a) $[Eu(acac)_3 \cdot PX]$ and b) $[Eu(dbm)_3 \cdot PX]$ complexes recorded at 300 and 77 K, under excitations at the $S_0 \rightarrow S_1$ transitions of the ligands (313; 418 nm – dbm and 323; 410 nm – acac), and also in the 4f–4f transitions of the Eu^{3+} ion.

Table 1
Experimental values of Intensity parameters (Ω_λ), the ratio between the $^5D_0 \rightarrow {}^7F_0$ and $^5D_0 \rightarrow {}^7F_2$ transition intensities (R_{02}), radiative (A_{rad}), non-radiative (A_{nrad}) rates and emission lifetime (τ), intrinsic emission efficiency (Q_{Ln}^{Ln}) of the $^5D_0$ emitting level, determined for the of $[Eu(acac)_3 \cdot PX]$ and $[Eu(dbm)_3 \cdot PX]$ complexes based on the emission spectra recorded at 300 K

Complexes	$\lambda_{exc.}$ (nm)	Ω_2 (10^{-20}cm^2)	Ω_4 (10^{-20}cm^2)	A_{rad} (s^{-1})	A_{nrad} (s^{-1})	A_{tot} (s^{-1})	τ (ms)	Q_{Ln}^{Ln} (%)
$[Eu(acac)_3(H_2O)_3]$[a]	394	29	13	1127	2523	3650	0.274	31
$[Eu(acac)_3 \cdot PX]$	410	11	5	465	10,320	10,750	0.093	4
	394	16	7	648	8876	9524	0.105	7
	323	16	6	608	7940	8547	0.117	7
$[Eu(dbm)_3(H_2O)]$[b]	394	37	4	716	2129	2845	0.351	25
$[Eu(dbm)_3 \cdot PX]$	418	29	8	1046	2475	3521	0.284	30
	394	21	8	801	1694	2695	0.175	30
	313	27	8	975	2947	3922	0.255	25

[a] Ref. [38].
[b] Ref. [39].

observe that the $[Eu(acac)_3 \cdot PX]$ complex (Fig. 5a) shows four main steps of mass loss. Where the first step of mass loss is about 10% from 40 to 170 °C, that can be due to desorption of physically adsorbed water and residual solvent, without any decomposition of the chemical bonds in the complex. The second step of mass loss (about 4.0%) between 170 and 220 °C is attributed to the loss of the PX ligand [37]. In the third step, in the temperature interval 230–350 °C, there is a strong endothermic peak centered at 270 °C, which is due to the loss of the β-diketones. Finally, when the temperature reaches beyond 400 °C, further decomposition of organic ingredients like acac and degradation of the PX occurred [9].

Furthermore, in the TG curve of the $[Eu(acac)_3 \cdot PX]$ (Fig. 5a), the mass losses in the temperature intervals of 40–250, 250–500, and 500–900 °C are 5%, 45%, and 5%, respectively. This thermal behavior can be assigned to the removal of solvent and thermal decomposition of the $[Eu(acac)_3 \cdot PX]$ complex, which is in good agreement with the DTG results. It should be noted that the total mass loss is about 60% and the TG/DTG data of $[Eu(dbm)_3 \cdot PX]$ complex (Fig. 5b) are similar to $[Eu(acac)_3 \cdot PX]$, except for total mass loss that is about 90% (Fig. 5).

4. Photoluminescence properties

4.1. Excitation spectral analysis

The excitation spectra of the $[Eu(dbm)_3 \cdot PX]$ and $[Eu(acac)_3 \cdot PX]$ complexes (Fig. 6) were recorded in the range of 250–590 nm at room (300K) and in liquid nitrogen (77K) temperatures, with the emission monitored in the $^5D_0 \rightarrow {}^7F_2$ transition of the Eu^{3+} ion, at ~614 and ~615nm respectively. The narrow absorption lines around 393, 460, 525, and 579nm are characteristic transitions of the Eu^{3+} ion corresponding to the $^7F_0 \rightarrow {}^5L_6$, $^7F_0 \rightarrow {}^5D_2$, $^7F_0 \rightarrow {}^5D_1$, and $^7F_0 \rightarrow {}^5D_0$ transitions, respectively. The broad absorption bands in the range from 250 to 500nm, arising from the β-diketonate group, are overlapped with those narrow bands from the Eu^{3+} ion attributed to the $^7F_0 \rightarrow {}^5D_4$, $^7F_0 \rightarrow {}^5L_7$, and $^7F_0 \rightarrow {}^5D_3$ transitions. The broad band contribution increases due to the absorption by the PX ligand [9].

These broad absorption bands (Fig. 6) are assigned to the centered $S_0 \rightarrow S_1$ β-diketonate and PX ligand transitions. This result indicates that the luminescence of the Eu^{3+}–β-diketonate-PX complexes is a consequence of the sensitization of the europium excited state by intramolecular non-radiative energy transfer from these two organic ligands including intermolecular energy transfer between these two

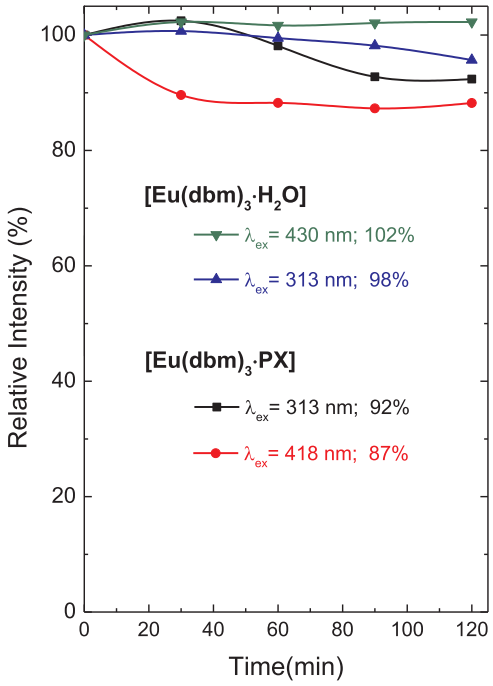

Fig. 8. Photostability curves of the [Eu(dbm)$_3$·(H$_2$O)] (excitation at 313 and 430 nm) and [Eu(dbm)$_3$·PX] (excitation at 313 and 418 nm) by monitoring the integrated area of to the $^5D_0 \rightarrow {}^7F_2$ transition of the Eu^{3+} ion. All curves were recorded at room temperature under irradiation with a 450 W Xenon lamp.

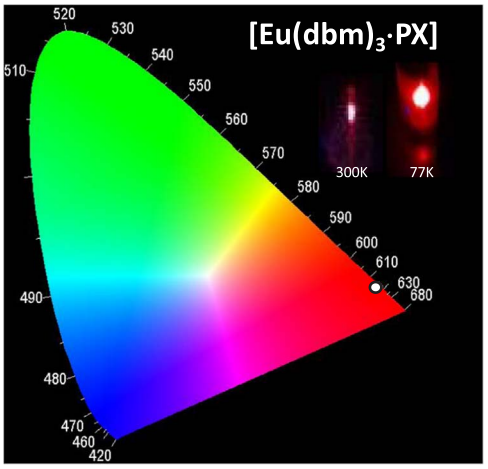

Fig. 9. CIE chromaticity diagram showing the x,y emission color coordinates for the [Eu(dbm)$_3$·PX] complex based on the emission spectra at different temperatures (300 K and 77 K) and excitation wavelengths. The inset figures are photographs of the [Eu(dbm)$_3$·PX] materials taken with a digital camera displaying the red emission under UV irradiation at 300 and 77 K.

ligands. The excitation spectra of the complexes containing the piroxicam ligand are quite different from the spectra of the other complexes (for example [Eu(dbm)$_3$L], [Eu(acac)$_3$L]: L= Phen, H$_2$O), indicating a higher disturbance caused by this ligand in comparison with the hydrated complexes, probably because of steric effects [38–40]. Upon careful observations, it may be noted that both excitation spectra of the complexes become broader, which could be ascribed to structural and modification of the phonon density of states.

4.2. Emission data

The emission spectra of the [Gd(acac)$_3$·PX] and [Gd(dbm)$_3$·PX] complexes (Fig. 1a and b, Support information) exhibit intense broad bands at about 395 and 458 nm assigned to the phosphorescence from $T_1 \rightarrow S_0$ transition, based on the zero phonon transitions of the acac and dbm ligands.

The emission spectra of the [Eu(acac)$_3$·PX] and [Eu(dbm)$_3$·PX] complexes (Fig. 7) were recorded at 300 and 77 K in the range of 450–750 nm. In both emission spectra, characteristic emission peaks of the Eu^{3+} ion are observed and which are assigned to the transitions $^5D_0 \rightarrow {}^7F_0$ (~ 582 nm), $^5D_0 \rightarrow {}^7F_1$ (~ 596 nm), $^5D_0 \rightarrow {}^7F_2$ (~ 614 nm), $^5D_0 \rightarrow {}^7F_3$ (653 nm), and $^5D_0 \rightarrow {}^7F_4$ (~ 706 nm), with the $^5D_0 \rightarrow {}^7F_2$ transition at 614 and 615 nm being the dominant emission peaks in the case of the dbm and acac ligands, respectively. The five expected transitions from the $^5D_0$ level are clearly observed in the $^5D_0 \rightarrow {}^7F_2$ transition and are responsible for the red emission of these coordination compounds. The presence of only one peak in the $^5D_0 \rightarrow {}^7F_0$ transition indicates the C_{nv}, C_n, or C_s symmetries in the local chemical environment of the Eu^{3+} ions. The $^5D_0 \rightarrow {}^7F_1$ transition is a magnetic dipole allowed transition, and is, therefore, practically insensitive to the local structural environment, and is generally taken as a reference. Thus, the intensity (the integration of the luminescence band) ratio of the $^5D_0 \rightarrow {}^7F_2$ transition to the $^5D_0 \rightarrow {}^7F_1$ transition can be used as a reference to conjectures about different chemical environments of the europium ion in the complexes, that is, it can be used as an indicator of the Eu^{3+} type of local site symmetry [41].

It is observed that the Eu^{3+} complexes with the ancillary PX ligand do not exhibit higher luminescence intensities in comparison with the hydrated complex (Fig. 7). This is understandable due to a possible strong vibrational coupling of the PX mode at 3334 cm^{-1} with the energy difference between the $^5D_0$ and $^7F_6$ levels of the Eu^{3+} ion (four-phonon multiphonon decay). On the other hand, one of the main features to be outlined from the photoluminescence spectra for the [Eu(dbm)$_3$·PX] complexes recorded at both 300 and 77 K is the absence of the broad emission bands due to the PX fluorescence or phosphorescence (Fig. 7b). This result indicates an efficient energy transfer from the ligand to the metal ion. Besides, all of these photoluminescence spectra display similar spectral profile, in which only intraconfigurational $4f^6$ transitions are observed, being dominated by the well-characterized $^5D_0 \rightarrow {}^7F_2$ transition allowed by the forced electric dipole mechanism. On the other hand, the emission spectral profiles of the [Eu(acac)$_3$·PX] complexes recorded at both 300 and 77 K are different, suggesting that there are structural exchanges in this complex at low temperature (77 K).

4.3. Experimental intensity parameters

The experimental intensity parameters (Ω_λ, λ = 2 and 4) were calculated from the emission spectra of [Eu(acac)$_3$·PX] and [Eu(dbm)$_3$·PX] complexes based on the $^5D_0 \rightarrow {}^7F_{2,4}$ electronic transitions and the $^5D_0 \rightarrow {}^7F_1$ magnetic dipole allowed transition as the reference. These parameters are calculated using coefficients of spontaneous emission, A_{0J}, given by Eq. (1):

$$A_{0J} = \frac{4e^2\omega^3}{3\hbar c^3}\chi \sum_{\lambda} \Omega_\lambda \langle {}^7F_J \| U^{(\lambda)} \| {}^5D_0 \rangle^2 \quad (1)$$

where λ = 2 and 4, e is the electronic charge, ω is the angular frequency of the transition, ħ is Planck's constant, c is the velocity of light, χ is the Lorentz local field correction term, given by $\chi = [n(n^2 + 2)^2]/9$, and $\langle {}^7F_J \| U^{(\lambda)} \| {}^5D_0 \rangle^2$ is a squared reduced matrix element whose value is 0.0032 for the $^5D_0 \rightarrow {}^7F_2$ transition and 0.0023 for the $^5D_0 \rightarrow {}^7F_4$ one [35]. The index of refraction n has been assumed equal to 1.5 (average index of refraction of these materials) [16,23,42].

Furthermore, it is possible to determine the intrinsic emission efficiency (Q_{Ln}^{Ln}) of the $^5D_0$ emitting level of the of the europium ion according to Eq. (2) bellow

$$Q_{Ln}^{Ln} = \frac{A_{rad}}{A_{rad} + A_{nrad}} \quad (2)$$

The total decay rate, $A_{total} = 1/\tau = A_{rad} + A_{nrad}$, where $A_{rad} = \Sigma A_{0\rightarrow J}$ and A_{nrad} is the non-radiative rate from the $^5D_0$, respectively.

Table 1 presents the values of the experimental intensity parameters (Ω_λ) thus obtained, together with the other photophysical data for these compounds. The radiative (A_{rad}), non-radiative (A_{nrad}) rates and intrinsic emission efficiencies (Q_{Ln}^{Ln}) of the $^5D_0$ emitting level correspond to the [Eu(acac)$_3$·PX] and [Eu(dbm)$_3$·PX] compounds.

The intensity parameters values change when the water molecules are substituted by PX ligand and also with temperature, which indicate clearly a structural change (Table 1), once these parameters are sensitive to the structure and nature of the chemical environment around the lanthanide ion.

The Eu^{3+} complexes present a substantially high dependence of A_{nrad} with the temperature. As a result, the intrinsic emission efficiency (Q_{Ln}^{Ln}) for the Eu^{3+} β-diketonate-PX complexes at low temperature at the same excitation when compared with 300 K are at least the double of the value at room temperature (see Table 1). This shows the extreme dependence of the emission efficiency with the excitation frequency, in accordance with the analysis performed in reference [43]. Moreover, the spectroscopic results in Table 1 indicate that not all organic ligands may improve luminescence efficiency, depending on the excitation wavelength [44]. Indeed, this is a point that should be carefully discussed when discussing intrinsic emission efficiency (η or Q_{Ln}^{Ln}) or emission quantum yields (q or Q_{Ln}^{L}).

The relatively shorter lifetime (τ) observed for the [Eu(acac)$_3$·PX] and [Eu(dbm)$_3$·PX] compounds in the solid state at room temperature and 394 nm excitation, may be attributed to the nonradiative transition process that is associated with vibronic coupling, being clearly different in the two cases. At the moment, we do not have a satisfactory explanation for this observation. The $^5D_0$ (Eu^{3+}) lifetimes were obtained from the luminescent decay profiles for the complexes at 300 and 77 K temperatures (see Table S1, Support information). It was found that the luminescence decay profiles obeyed a second order exponential decay at 300 K and a single exponential decay at the liquid nitrogen temperature.

We have checked the photostability curves of these novel compounds. The compounds with the β-diketonate (dbm) ligand and H_2O and PX ancillary ligands have presented good photostability in comparison with the compounds with the β-diketonate acac ligand [45]. Fig. 8 shows the cases for the dbm and H_2O and PX ancillary ligands. It is noteworthy the photo stability of these compounds at different excitation wavelengths by using a 450 W Xenon lamp (much more intense than the UV radiation from the Sun). We, therefore, conclude that under UV Sun exposure their stability should be even better.

The question (mechanisms) of degradation, under UV (A, B or C) excitation of Ln^{3+} β-diketonates ligands, with ancillary ligands, is still an open question. However, at least in the present case, we conclude that the present novel complexes, with ancillary ligands, maintain their photostability even under high intensity UV-blue irradiation.

The CIE chromaticity coordinates ($x = 0.684$, $y = 0.314$) generated from the emission spectrum of and [Eu(dbm)$_3$·PX] under excitation at 418 nm (Fig. 9), indicating that the complex containing Eu^{3+} ions exhibits the monochromatic red emission color [46]. The inset in Fig. 9 are photographs of the [Eu(dbm)$_3$·PX] complex showing strong red emission for the complexes when registered at room and low temperature. All the other complexes present very similar chromaticity coordinate values.

5. Conclusion

Two novel luminescent europium *tris*(*β*-diketonate) complexes containing piroxicam, as ancillary ligand, were synthesized. These complexes exhibited red sharp emission at ~ 614 nm, typical from the Eu^{3+} ion, from which photophysical parameters could be determined such: intensity parameters, lifetimes, radiative and non-radiative transition values as well as intrinsic emission efficiencies. According to the characterization techniques employed, and thermal and photoluminescence analyses, from the luminescence studies, we found that the molecular structure of PX ligand greatly affect the absorption and emission intensities of these europium *tris*(*β*-diketonate) complexes. In addition, they show an extremely high dependence with the excitation wavelength, as predicted in Ref. [44], and the temperature maintains their thermal stability. We have also shown that these coordination compounds, besides being thermal stable, present a good photostability in comparison with previous β-diketonate compounds with different compositions.

Acknowledgments

This research is supported by grants from the Brazilian funding agencies, Conselho Nacional de Desenvolvimento Científico e Tecnológico (CNPq), INCT-INAMI (CNPq), Coordenação de Aperfeiçoamento de Pessoal de Nível Superior (CAPES), Rede Nanobiotech and Fundação de Amparo à Pesquisa do Estado de São Paulo (FAPESP).

Appendix A. Supporting information

Supplementary data associated with this article can be found in the online version at http://dx.doi.org/10.1016/j.jlumin.2017.09.029.

References

[1] V.I. Verlan, M.S. Iovu, I. Culeac, Y.H. Nistor, C.I. Turta, V.E. Zubareva, J. Optoelec. Adv. Macromol. 13 (2011) 1590.
[2] J.-C.G. Bunzli, C. Piguet, Chem. Soc. Rev. 34 (2005) 1048.
[3] C.M.G. Santos, A.J. Harte, S.J. Quinn, T. Gunnlaugsson, Coord. Chem. Rev. 252 (2008) 2512.
[4] R. Reisfeld, C.K. Jørgensen, Lasers and excited states of rare earths, in: Inorganic Chemistry Concepts 1, 1977, Springer-Verlag Berlin, Heidelberg.
[5] R. Reisfeld, Opt. Mater. 32 (2010) 850.
[6] R. Reisfeld, D. Shamrakov, C.K. Jorgensen, Solar Energy Materials and Solar Cells 33 (1994) 417.
[7] R. Reisfeld, B. Jasinska, V. Levchenko, M. Gorgol, T. Saraidarov, I. Popov, T. Antropova, E. Rysiakiewicz-Pasek, J. Lumin. 169 (2016) 440.
[8] R. Reisfeld, V. Levchenko, F. Piccinelli, M. Bettinelli, J. Lumin. 170 (2016) 820.
[9] G.F. de Sá, O.L. Malta, C.D. Donega, A.M. Simas, R.L. Longo, P.A. Santa-Cruz, E.F. Silva, Coord. Chem. Rev. 196 (2000) 165.
[10] D.F. Parra, A. Mucciolo, D.G. Duarte, H.F. Brito, A.B. Lugão, J. Appl. Poly. Sci. 100 (2006) 406.
[11] N. Sabbatini, M. Guardingli, Coord. Chem. Rev. 123 (1993) 201.
[12] M.C.F. Cunha, H.F. Brito, L.B. Zinner, G. Vicentini, A.B. Nascimento, Coord. Chem. Rev. 196 (2000) 165.
[13] Y.J. Gu, B. Yan, Y.Y. Li, J. Sol. Stat. Chem. 190 (2012) 36.
[14] J.-C.G. Bünzli, G.R. Choppin, Lanthanide Probes in Life, Chemical and Earth Sciences Theory and Practice, Elsevier, Amsterdam, 1989.
[15] F.S. Richardson, Chem. Rev. 82 (1982) 541.
[16] Y. Liu, Y. Wang, J. He, Q. Mei, K. Chen, J. Cui, C. Li, M. Zhu, J. Peng, W. Zhu, Y. Cao, Org. Electronics 13 (2012) 1038.
[17] E.E.S. Teotonio, H.F. Brito, G.F. de Sá, M.C.F.C. Felinto, R.H. Santos, R.M. Fuquen, I.F. Costa, A.R. Kennedy, D.G. Gilmore, W.M. Faustino, Polyhedron 38 (2012) 58.
[18] S. Linfang, L. Yanwei, C. Huaru, G. Ying, M.A. Yongchun, J. Rare Earths 30 (2012) 17.
[19] J.E. Weder, C.T. Dillon, T.W. Hambley, B.J. Kennedy, P.A. Lay, J.R. Biffin, H.L. Regtop, N.M. Davies, Coord. Chem. Rev. 232 (2002) 95.
[20] M.A. Zayed, F.A. Nour El-Dien, G.G. Mohamed, N.A. El-Gamel, Spectrochimica Acta Part A 64 (2006) 216.
[21] S.M.Z.O. Al-Kindy, F.E. Suliman, A.A. Al-Wishahi, H.A.J. Al-Lawati, M. Aoudia, J. Lumin. 127 (2007) 291.
[22] S.M.Z.O. Al-Kindy, A.O. Al-Wishahi, F.E. Suliman, Talanta 64 (2004) 1343.
[23] H.F. Brito, O.L. Malta, M.C.F.C. Felinto, E.E.S. Teotonio, Patai Series; the chemistry of functional groups – the chemistry of metal enolates, in: J. Zabicky (Ed.), Luminescence Phenomena Involving Metal Enolate, John Wiley & Sons Ltd, West Sussex, England, 2009, pp. 131–184 (Part 1).
[24] J. Kai, M.C.F.C. Felinto, L.A.O. Nunes, O.L. Malta, H.B. Brito, J. Mater. Chem. *21* (2011) *3796*.
[25] R.P. Aquino, G. Auriemma, M. d'Amore, A.M. D'Ursi, T. Mencherini, P.D. Gaudio, Carbohydrate Polymers 89 (2012) 740.
[26] F. Enrichi, R. Ricco, P. Scopece, A. Parma, A.R. Mazaheri, P. Riello, A. Benedetti, J. Nanopart. Res. 12 (2010) 1925.
[27] E. Niyama, H.F. Brito, M. Cremona, E.E.S. Teotonio, R. Reyes, G.E.S. Brito, M.C.F.C. Felinto, Spectrochimica Acta Part A 61 (2005) 2643.
[28] K. Nakamoto, Infrared and Raman Spectra of Inorganic Coordination Compounds.

Wiley, New York, 1968.
[29] T. Miyazawa, T. Shimanouchi, S. Mizushima, J. Chem. Phys. 29 (1958) 611.
[30] D.X. West, J.K. Swearingen, J.V. Martinez, S.H. Ortega, A.K. El- Sawaf, F.V. Meurs, A. Castineiras, I. Garcia, E. Bermejo, Polyhedron 18 (1999) 2919.
[31] R. Cini, G. Giorgi, A. Cinquantini, C. Rossi, M. Sabat, Inorg. Chem. 29 (1990) 5197.
[32] S.Z. Haider, K.M.A. Malik, J. Bangladesh Acad. Sci. 6 (1982) 119125.
[33] E.G. Ferrer, S.B. Etcheverry, E.J. Baran, Monatch. Chem. 124 (1993) 355.
[34] M.A. Zayed, F.A. Nou–r El-Dien, G.G. Mohamed, N.E.A. El-Gamel, Spectrochimica Acta Part A 64 (2006) 216.
[35] J.T. Zaharieva, M.M. Milanova, D.S. Todorovsky, Cent. Eur. J. Chem. 9 (2011) 290.
[36] A.K. Singh, S.K. Singh, H. Mishra, R. Prakash, S.B. Rai, J. Phys. Chem. B 114 (2010) 13042.
[37] H.E. Grandelli, J.C. Hassler, The J. Supercritical Fluids **71** (2012) 19.
[38] E.B. Gibelli, Preparação e caracterização de dispositivos eletroluminescentes de complexos de β-dicetonatos de íons Tb3+, Eu3+, Gd3+ com ligantes macrocíclicos e filmes de UO_2^{2} (Master dissertation), University of São Paulo-USP, São Paulo, Brazil, 2010.
[39] E.E.S. Teotonio, – Síntese e investigação das propriedades fotoluminescentes de dispositivos moleculares conversores de luz (DMCL) de complexos dicetonatos de terras raras com ligantes amidas, Doctorate Thesis University of São Paulo-USP, São Paulo, Brazil, 2004.
[40] E.E.S. Teotonio, H.F. Brito, G.F. de Sá, M.C.F.C. Felinto, R.H. Santos, R.M. Fuquen, I.F. Costa, A.R. Kennedy, D.G. Gilmore, W.M. Faustino, Polyhedron 38 (2012) 58.
[41] S. Qi, W. Yin, J. Mater. Sci. 46 (2011) 5288.
[42] W.T. Carnall, H. Crosswhile, Energy Levels Structure and Transition Probabilities of the Trivalent Lanthanides in LaF_3, Argonne National Laboratory, United States, 1977.
[43] M. Bettinelli, A.; F. Piccinelli, A.N.C. Neto, O.L. Malta, J. Lumin 131 (2011) 1026.
[44] R.A.S. Ferreira, M. Nolasco, A.C. Roma, R.L. Longo, O.L. Malta, L.D. Carlos, Chemistry A European Journal 18 (2012) 12130.
[45] J. Kai, M.C.F.C. Felinto, L.A.O. Nunes, O.L. Malta, H.F. Brito, J. Mater. Chem. 21 (2011) 3796.
[46] P.A.Santa-Cruz, F.S.Teles, Spectra Lux Software v.2.0 Beta, Ponto Quântico Nanodispositivos, RENAMI, 2003.